

## Research Article

# A Fast LMMSE Channel Estimation Method for OFDM Systems

Wen Zhou and Wong Hing Lam

*Department of Electrical and Electronics Engineering, The University of Hong Kong, Hong Kong*

Correspondence should be addressed to Wen Zhou, wenzhou@eee.hku.hk

Received 20 July 2008; Revised 10 January 2009; Accepted 20 March 2009

Recommended by Lingyang Song

A fast linear minimum mean square error (LMMSE) channel estimation method has been proposed for Orthogonal Frequency Division Multiplexing (OFDM) systems. In comparison with the conventional LMMSE channel estimation, the proposed channel estimation method does not require the statistic knowledge of the channel in advance and avoids the inverse operation of a large dimension matrix by using the fast Fourier transform (FFT) operation. Therefore, the computational complexity can be reduced significantly. The normalized mean square errors (NMSEs) of the proposed method and the conventional LMMSE estimation have been derived. Numerical results show that the NMSE of the proposed method is very close to that of the conventional LMMSE method, which is also verified by computer simulation. In addition, computer simulation shows that the performance of the proposed method is almost the same with that of the conventional LMMSE method in terms of bit error rate (BER).

Copyright © 2009 W. Zhou and W. H. Lam. This is an open access article distributed under the Creative Commons Attribution License, which permits unrestricted use, distribution, and reproduction in any medium, provided the original work is properly cited.

## 1. Introduction

Orthogonal frequency division multiplexing (OFDM) is an efficient high data rate transmission technique for wireless communication [1]. OFDM presents advantages of high spectrum efficiency, simple and efficient implementation by using the fast Fourier transform (FFT) and the inverse Fast Fourier Transform (IFFT), mitigation of intersymbol interference (ISI) by inserting cyclic prefix (CP), and robustness to frequency selective fading channel. Channel estimation plays an important part in OFDM systems. It can be employed for the purpose of detecting received signal, improving the capacity of orthogonal frequency division multiple access (OFDMA) systems by cross-layer design [2], and improving the system performance in terms of bit error rate (BER) [3–5].

*1.1. Previous Work.* The present channel estimation methods generally can be divided into two kinds. One kind is based on the pilots [6–9], and the other is blind channel estimation [10–12] which does not use pilots. Blind channel estimation methods avoid the use of pilots and have higher spectral efficiency. However, they often suffer from high computation complexity and low convergence speed since they often need a large amount of receiving data to obtain some statistical

information such as cyclostationarity induced by the cyclic prefix. Therefore, blind channel estimation methods are not suitable for applications with fast varying fading channels. And most practical communication systems such as World Interoperability for Microwave Access (WIMAX) system adopt pilot assisted channel estimation, so this paper studies the first kind.

For the pilot-aided channel estimation methods, there are two classical pilot patterns, which are the block-type pattern and the comb-type pattern [4]. The block-type refers to that the pilots are inserted into all the subcarriers of one OFDM symbol with a certain period. The block-type can be adopted in slow fading channel, that is, the channel is stationary within a certain period of OFDM symbols. The comb-type refers to that the pilots are inserted at some specific subcarriers in each OFDM symbol. The comb-type is preferable in fast varying fading channels, that is, the channel varies over two adjacent OFDM symbols but remains stationary within one OFDM symbol. The comb-type pilot arrangement-based channel estimation has been shown as more applicable since it can track fast varying fading channels, compared with the block-type one [4, 13]. The channel estimation based on comb-type pilot arrangement is often performed by two steps. Firstly, it estimates the channel frequency response on all pilot

subcarriers, by least square (LS) method, LMMSE method, and so on. Secondly, it obtains the channel estimates on all subcarriers by interpolation, including data subcarriers and pilot subcarriers in one OFDM symbol. There are several interpolation methods including linear interpolation method, second-order polynomial interpolation method, and phase-compensated interpolation [4].

In [14], the linear minimum mean square error (LMMSE) channel estimation method based on channel autocorrelation matrix in frequency domain has been proposed. To reduce the computational complexity of LMMSE estimation, a low-rank approximation to LMMSE estimation has been proposed by singular value decomposition [6]. The drawback of LMMSE channel estimation [6, 14] is that it requires the knowledge of channel autocorrelation matrix in frequency domain and the signal to noise ratio (SNR). Though the system can be designed for fixed SNR and channel frequency autocorrelation matrix, the performance of the OFDM system will degrade significantly due to the mismatched system parameters. In [15], a channel estimation exploiting channel correlation both in time and frequency domain has been proposed. Similarly, it needs to know the channel autocorrelation matrix in frequency domain, the Doppler shift, and SNR in advance. Mismatched parameters of the Doppler shift and the delay spread will degrade the performance of the system [16]. It is noted that the channel estimation methods proposed in [6, 14–16] can be adopted in either the block-type pilot pattern or the comb-type pilot pattern.

When the assumption that the channel is time-invariant within one OFDM symbol is not valid due to high Doppler shift or synchronization error, the intercarrier interference (ICI) has to be considered. Some channel estimation and signal detection methods have been proposed to compensate the ICI effect [17, 18]. In [17], a new equalization technique to suppress ICI in LMMSE sense has been proposed. Meanwhile, the authors reduced the complexity of channel estimator by using the energy distribution information of the channel frequency matrix. In [18], the authors proposed a new pilot pattern, that is, the grouped and equispaced pilot pattern and corresponding channel estimation and signal detection to suppress ICI.

**1.2. Contributions.** In this paper, the OFDM system framework based on comb-type pilot arrangement is adopted, and we assume that the channel remains stationary within one OFDM symbol, and therefore there is no ICI effect. We propose a fast LMMSE channel estimation method. The proposed method has three advantages over the conventional LMMSE method. Firstly, the proposed method does not require the knowledge of channel autocorrelation matrix and SNR in advance but can achieve almost the same performance with the conventional LMMSE channel estimation in terms of the normalized mean square error (NMSE) of channel estimation and bit error rate (BER). Secondly, the proposed method needs only fast Fourier transform (FFT) operation instead of the inversion operation of a large dimensional matrix. Therefore, the computational

complexity can be reduced significantly, compared with the conventional LMMSE method. Thirdly, the proposed method can track the changes of channel parameters, that is, the channel autocorrelation matrix and SNR. However, the conventional LMMSE method cannot track the channel. Once the channel parameters change, the performance of the conventional LMMSE method will degrade due to the parameter mismatch.

**1.3. Organization.** The paper is organized as follows. Section 2 describes the OFDM system model. Section 3 describes the proposed fast LMMSE channel estimation. We analyze the mean square error (MSE) of the proposed fast LMMSE channel estimation and the MSE of the conventional LMMSE channel estimation in Section 4. The simulation results and numerical results of the proposed algorithm are discussed in Section 5 followed by conclusion in Section 6.

## 2. System Model

The OFDM system model with pilot signal (i.e., training sequence) assisted is shown in Figure 1. For  $N$  subcarriers in the OFDM system, the transmitted signal  $x(i, n)$  in time domain after inverse Fast Fourier Transform (IFFT) is given by

$$x(i, n) = \text{IFFT}_N[X(i, k)] = \frac{1}{N} \sum_{k=0}^{N-1} X(i, k) \exp\left\{\frac{j2\pi nk}{N}\right\}, \quad (1)$$

where  $X(i, k)$  denotes the transmitted signal in frequency domain at the  $k$ th subcarrier in the  $i$ th OFDM symbol. The comb-type pilot pattern [4] is adopted in this paper. The pilot subcarriers are equispaced inserted into each OFDM symbol. It is assumed that the number of the total pilot subcarriers is  $N_p$ , and the inserting gap is  $R$ . Each OFDM symbol is composed of the pilot subcarriers and the data subcarriers. It is assumed that the index of the first pilot subcarrier is  $k_0$ . Therefore, the set of the indices of pilot subcarriers,  $\eta$ , can be written as

$$\eta = \{k \mid k = mR + k_0, m = 0, 1, \dots, N_p - 1\}, \quad (2)$$

where  $k_0 \in [0, R)$ . The received signal  $Y(i, k)$  in frequency domain after FFT can be written as

$$Y(i, k) = X(i, k)H(i, k) + W(i, k), \quad (3)$$

where  $W(i, k)$  denotes the AGWN with zero mean, and variance  $\sigma_w^2$ ,  $H(i, k)$  is the frequency response of the radio channel at the  $k$ th subcarrier of the  $i$ th OFDM symbol. Then, the received pilot signal  $Y_p(i, k)$  is extracted from  $Y(i, k)$  to perform channel estimation. As shown in Figure 2, the channel estimator firstly performs channel frequency response estimation at pilot subcarriers. There are some channel estimation methods for this part such as LS and LMMSE estimator [4]. Next, once the channel frequency response estimation at pilot subcarriers,  $\tilde{H}_p(i, k)$ , is obtained, the estimator performs interpolation to obtain channel frequency response estimation at all subcarriers. There

are linear interpolation method [4], second-order polynomial interpolation method [4], discrete Fourier transform-(DFT-) based interpolation method [19], and so on. In our system model, the linear interpolation method is adopted. After channel estimation, maximum likelihood detection is performed to obtain the estimated frequency signal  $\tilde{X}(i, k)$ . The  $\tilde{X}(i, k)$  is given by

$$\tilde{X}(i, k) = \underset{S}{\operatorname{argmin}} \left| Y(i, k) - \tilde{H}(i, k)S \right|^2, \quad (4)$$

where  $S \in s$ , and  $s$  is the set containing all constellation points, which depends on modulation method, that is, the signal mapper. For instance, if QPSK modulation is adopted, the set  $s = \{(1/\sqrt{2})(1 + j), (1/\sqrt{2})(1 - j), (1/\sqrt{2})(-1 + j), (1/\sqrt{2})(-1 - j)\}$ . Finally, the estimated frequency signal  $\tilde{X}(i, k)$  passes through the signal demapper to obtain the received bit sequence.

### 3. The Proposed Fast LMMSE Algorithm

*3.1. Properties of the Channel Correlation Matrix in Frequency Domain.* The channel impulse response in time domain can be expressed as

$$h(i, n) = \sum_{l=0}^{L-1} h_l(i) \delta(n - \tau_l), \quad (5)$$

where  $h_l(i)$  is the complex gain of the  $l$ th path in the  $i$ th OFDM symbol period,  $\delta(\cdot)$  is the Kronecker delta function,  $\tau_l$  is the delay of the  $l$ th path in unit of sample point, and  $L$  is the number of resolvable paths. Assume that different paths  $h_l(i)$  are independent from each other and the power of the  $l$ th path is  $\sigma_l^2$ . The channel is normalized so that  $\sigma_h^2 = \sum_l \sigma_l^2 = 1$ . The channel response in frequency domain  $H(i, k)$  is the FFT of  $h(i, n)$ , and it is given by

$$H(i, k) = \operatorname{FFT}_N(h(i, n)) = \sum_{m=0}^{N-1} h(i, m) \exp\left\{-\frac{j2\pi mk}{N}\right\}, \quad (6)$$

where  $\operatorname{FFT}_N(\bullet)$  denotes  $N$  points FFT operation. The channel autocorrelation matrix in frequency domain can be expressed as

$$\begin{aligned} R_{HH}(m, n) &= E[H(i, m)H^*(i, n)] \\ &= E\left[\sum_{k=0}^{N-1} h(i, k) \exp\left\{-\frac{j2\pi km}{N}\right\} \cdot \sum_{k=0}^{N-1} h^*(i, k) \exp\left\{\frac{j2\pi kn}{N}\right\}\right] \\ &= \sum_{k=0}^{N-1} E\{|h(i, k)|^2\} \exp\left\{-\frac{j2\pi k(m-n)}{N}\right\} \\ &= \sum_{l=0}^{L-1} \sigma_l^2 \exp\left\{-\frac{j2\pi \tau_l(m-n)}{N}\right\}, \end{aligned} \quad (7)$$

where  $E(\bullet)$  denotes expectation. Denote the vector form of the channel autocorrelation matrix by  $\mathbf{R}_{HH}$ , and we have  $\mathbf{R}_{HH} = [R_{HH}(i, j)]_{N \times N}$ . It is easy to find that the matrix  $\mathbf{R}_{HH}$  is a circulant matrix. Therefore, as in [20], the eigenvalues of  $\mathbf{R}_{HH}$  are given by

$$\begin{aligned} &[\lambda_0 \ \lambda_1 \ \cdots \ \lambda_{N-1}] \\ &= [\operatorname{FFT}_N(R_{HH}(0, 0) \ R_{HH}(0, 1) \ \cdots \ R_{HH}(0, N-1))]. \end{aligned} \quad (8)$$

The formula (8) can be equivalently written as

$$\lambda_k = \sum_{n=0}^{N-1} R_{HH}(0, n) \exp\left\{-\frac{j2\pi nk}{N}\right\}, \quad k = 0, 1, \dots, N-1. \quad (9)$$

We can easily obtain from (7) and (9) that the number of nonzero eigenvalues of  $\mathbf{R}_{HH}$  is equal to the total number of resolvable paths,  $L$  (see Appendix A). It is known by us that the rank of a square matrix is the number of its nonzero eigenvalues. Therefore the rank of  $\mathbf{R}_{HH}$  is  $L$ , and  $\mathbf{R}_{HH}$  is a singular matrix since  $L < N$ . The matrix  $\mathbf{R}_{HH}$  does not have the inverse matrix and has only the Moore-Penrose inverse matrix. However, the rank of the matrix  $\mathbf{R}_{HH} + \sigma_w^2 \mathbf{I}$  is  $N$  (see Appendix A), where  $\mathbf{I}$  is an  $N$  by  $N$  identity matrix. Therefore, the matrix  $\mathbf{R}_{HH} + \sigma_w^2 \mathbf{I}$  is not singular and has the inverse matrix.

*3.2. The Proposed Fast LMMSE Channel Estimation Algorithm.* Let

$$\mathbf{H}_p(i) = [H_p(i, 0) \ H_p(i, 1) \ \cdots \ H_p(i, N_p - 1)]^T \quad (10)$$

denote the channel frequency response at pilot subcarriers of the  $i$ th OFDM symbol, and let

$$\mathbf{Y}_p(i) = [Y_p(i, 0) \ Y_p(i, 1) \ \cdots \ Y_p(i, N_p - 1)]^T \quad (11)$$

denote the vector of received signal at pilot subcarriers of the  $i$ th OFDM symbol after FFT. Denote the pilot signal of the  $i$ th OFDM symbol by  $X_p(i, j)$ ,  $j = 0, 1, \dots, N_p - 1$ . The channel estimate at pilot subcarriers based on least square (LS) criterion is given by

$$\begin{aligned} \tilde{\mathbf{H}}_{p,ls}(i) &= [\tilde{H}_{p,ls}(i, 0) \ \tilde{H}_{p,ls}(i, 1) \ \cdots \ \tilde{H}_{p,ls}(i, N_p - 1)]^T \\ &= \begin{bmatrix} Y_p(i, 0) & Y_p(i, 1) & \cdots & Y_p(i, N_p - 1) \\ X_p(i, 0) & X_p(i, 1) & \cdots & X_p(i, N_p - 1) \end{bmatrix}^T. \end{aligned} \quad (12)$$

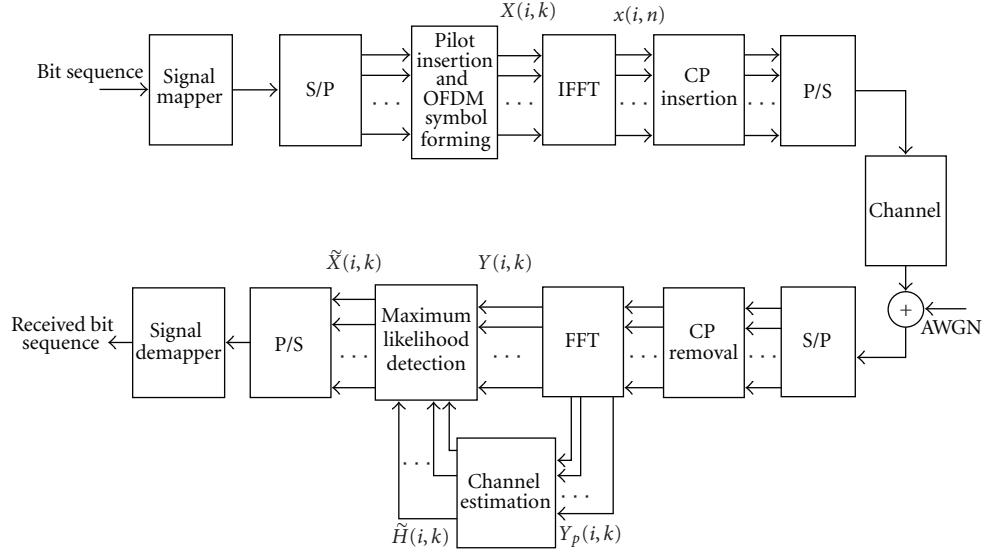


FIGURE 1: Baseband OFDM system.

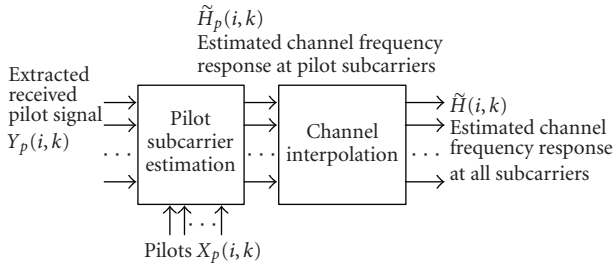


FIGURE 2: Channel estimation based on comb-type pilots.

The LMMSE estimator at pilot subcarriers is given by [6]

$$\begin{aligned} & \tilde{\mathbf{H}}_{p, \text{LMMSE}}(i) \\ &= \left[ \tilde{H}_{p, \text{LMMSE}}(i, 0) \quad \tilde{H}_{p, \text{LMMSE}}(i, 1) \quad \cdots \quad \tilde{H}_{p, \text{LMMSE}}(i, N_p - 1) \right] \\ &= \mathbf{R}_{\mathbf{H}_p \mathbf{H}_p} \left( \mathbf{R}_{\mathbf{H}_p \mathbf{H}_p} + \frac{\beta}{\text{SNR}} \mathbf{I} \right)^{-1} \tilde{\mathbf{H}}_{p, \text{LS}}(i), \end{aligned} \quad (13)$$

where  $\mathbf{R}_{\mathbf{H}_p \mathbf{H}_p}$  is channel autocorrelation matrix at pilot subcarriers and is defined by  $\mathbf{R}_{\mathbf{H}_p \mathbf{H}_p} = E\{\mathbf{H}_p \mathbf{H}_p^H\}$ , where  $(\cdot)^H$  denotes Hermitian transpose. It is easy to verify that the matrix  $\mathbf{R}_{\mathbf{H}_p \mathbf{H}_p}$  is circulant, the rank of  $\mathbf{R}_{\mathbf{H}_p \mathbf{H}_p}$  is equal to  $L$ , and the rank of  $\mathbf{R}_{\mathbf{H}_p \mathbf{H}_p} + \sigma_w^2 \mathbf{I}$  is equal to  $N_p$ . The signal-to-noise ratio (SNR) is defined by  $\text{SNR} = E|X_p(k)|^2 / \sigma_w^2$ , and  $\beta = E|X_p(k)|^2 E|1/X_p(k)|^2$  is a constant depending on the signal constellation. For 16QAM modulation  $\beta = 17/9$  and for QPSK and BPSK modulation  $\beta = 1$ . If the channel autocorrelation matrix  $\mathbf{R}_{\mathbf{H}_p \mathbf{H}_p}$  and SNR are known in advance,  $\mathbf{R}_{\mathbf{H}_p \mathbf{H}_p} (\mathbf{R}_{\mathbf{H}_p \mathbf{H}_p} + (\beta/\text{SNR})\mathbf{I})^{-1}$  needs to be calculated only once. However, the autocorrelation matrix

$\mathbf{R}_{\mathbf{H}_p \mathbf{H}_p}$  and SNR are often unknown in advance and time varying. Therefore the LMMSE channel estimator becomes unavailable in practice. To solve the problem, we propose the fast LMMSE channel estimation algorithm. The algorithm can be divided into three steps. The first step is to obtain the estimate of channel autocorrelation matrices  $\mathbf{R}_{\mathbf{H}_p \mathbf{H}_p}$  and  $\tilde{\mathbf{R}}_{\mathbf{H}_p \mathbf{H}_p}$ . Firstly, we obtain the least square (LS) channel estimation at pilot subcarriers in time domain,  $\tilde{h}_{p, \text{LS}}(i, k)$ , and it is given by

$$\tilde{h}_{p, \text{LS}}(i, k) = \frac{1}{N_p} \sum_{n=0}^{N_p-1} \tilde{H}_{p, \text{LS}}(i, n) \exp\left\{ \frac{j2\pi nk}{N_p} \right\}, \quad (14)$$

$$k = 0, 1, \dots, N_p - 1.$$

Secondly, the most significant taps (MSTs) algorithm [21] has been proposed to obtain the refined channel estimation in time domain. The MST algorithm deals with each OFDM symbol by reserving the most significant  $L'$  paths in terms of power and setting the other taps to be zero. The algorithm can reduce the influence of AWGN and other interference significantly, compared with the LS method. However, the algorithm may choose the wrong paths and omit the right paths because of the influence of AWGN and other interference. Thus, we will improve the algorithm of [21] by processing several adjacent OFDM symbols jointly. We calculate the average power of each tap for  $N_{\text{MST}}$  adjacent OFDM symbols,  $P_{\text{LS}}(k)$ , and it is given by

$$P_{\text{LS}}(k) = \frac{1}{N_{\text{MST}}} \sum_{i=0}^{N_{\text{MST}}-1} \left| \tilde{h}_{p, \text{LS}}(i, k) \right|^2, \quad k = 0, 1, \dots, N_p - 1. \quad (15)$$

Then we choose the  $L'$  most significant taps from  $P_{LS}(k)$  and reserve the indices of them into a set  $\alpha'$ . Finally, the refined channel estimation in time domain,  $\tilde{h}_{p,MST}$ , is given by

$$\begin{aligned} \tilde{h}_{p,MST}(i, k) &= \begin{cases} \tilde{h}_{p,ls}(i, k), & \text{if } k \in \alpha', \\ 0, & \text{if } k \notin \alpha', \end{cases} \\ k &= 0, 1, \dots, N_p - 1, \quad i = 0, 1, \dots, N_{MST} - 1. \end{aligned} \quad (16)$$

Denote the first row of the matrix  $\tilde{\mathbf{R}}_{H_p, H_p}$  by  $\tilde{\mathbf{A}}$ . Then  $\tilde{\mathbf{A}}$  can be given from (7) by

$$\tilde{\mathbf{A}} = N_p \cdot \text{IFFT}_{N_p}[\mathbf{P}_{MST}], \quad (17)$$

where  $\mathbf{P}_{MST}$  is a 1 by  $N_p$  vector with each entry

$$P_{MST}(k) = \begin{cases} P_{LS}(k), & \text{if } k \in \alpha', \\ 0, & \text{if } k \notin \alpha', \end{cases} \quad (18) \\ k = 0, 1, \dots, N_p - 1.$$

Since the matrix  $\tilde{\mathbf{R}}_{H_p, H_p}$  is circulant,  $\tilde{\mathbf{R}}_{H_p, H_p}$  can be acquired by circle shift of  $\tilde{\mathbf{A}}$ . The second step is to obtain the estimate of SNR. The estimate of SNR,  $\widehat{\text{SNR}}$ , is given by

$$\widehat{\text{SNR}} = \frac{\sum_k P_{MST}(k)}{\sum_k P_{LS}(k) - \sum_k P_{MST}(k)}. \quad (19)$$

The third step is to obtain the estimate of the matrix  $\mathbf{R}_{H_p, H_p}(\mathbf{R}_{H_p, H_p} + (\beta/\text{SNR})\mathbf{I})^{-1}$ ,  $\tilde{\mathbf{R}}_{H_p, H_p}(\tilde{\mathbf{R}}_{H_p, H_p} + (\beta/\widehat{\text{SNR}})\mathbf{I})^{-1}$ . We refer to the matrix  $\mathbf{R}_{H_p, H_p}(\mathbf{R}_{H_p, H_p} + (\beta/\text{SNR})\mathbf{I})^{-1}$  as the LMMSE matrix in this paper. Since  $\mathbf{R}_{H_p, H_p}$  is a circulant matrix and  $(\mathbf{R}_{H_p, H_p} + (\beta/\text{SNR})\mathbf{I})^{-1}$  is a circulant matrix, the product of  $\mathbf{R}_{H_p, H_p}$  and  $(\mathbf{R}_{H_p, H_p} + (\beta/\text{SNR})\mathbf{I})^{-1}$  is also a circulant matrix. Therefore, we need only to compute the estimate of the first row of the LMMSE matrix. Denote the first row of LMMSE matrix by  $\tilde{\mathbf{B}}$ . The estimate of  $\tilde{\mathbf{B}}$ ,  $\tilde{\tilde{\mathbf{B}}}$ , is given by (see Appendix B)

$$\begin{aligned} \tilde{\tilde{\mathbf{B}}} &= \text{IFFT}_{N_p} \left[ \begin{array}{c} \frac{P_{MST}(0)}{P_{MST}(0) + (\beta/N_p \widehat{\text{SNR}})} \frac{P_{MST}(1)}{P_{MST}(1) + (\beta/N_p \widehat{\text{SNR}})} \\ \dots \\ \frac{P_{MST}(N_p - 1)}{P_{MST}(N_p - 1) + (\beta/N_p \widehat{\text{SNR}})} \end{array} \right] \end{aligned} \quad (20)$$

where  $\text{IFFT}_{N_p}(\bullet)$  denotes  $N_p$  points IFFT operation. Therefore the estimated LMMSE matrix  $\tilde{\mathbf{R}}_{H_p, H_p}(\tilde{\mathbf{R}}_{H_p, H_p} + (\beta/\widehat{\text{SNR}})\mathbf{I})^{-1}$  can be obtained from circle shift of  $\tilde{\tilde{\mathbf{B}}}$ . The channel estimation in frequency domain at pilot subcarriers for the  $i$ th OFDM symbol can be given by

$$\begin{aligned} \tilde{H}_{p, \text{fast LMMSE}}(i) &= \tilde{\mathbf{R}}_{H_p, H_p} \left( \tilde{\mathbf{R}}_{H_p, H_p} + \frac{\beta}{\widehat{\text{SNR}}} \mathbf{I} \right)^{-1} \tilde{H}_{p,ls}(i), \\ i &= 0, 1, \dots, N_{MST} - 1. \end{aligned} \quad (21)$$

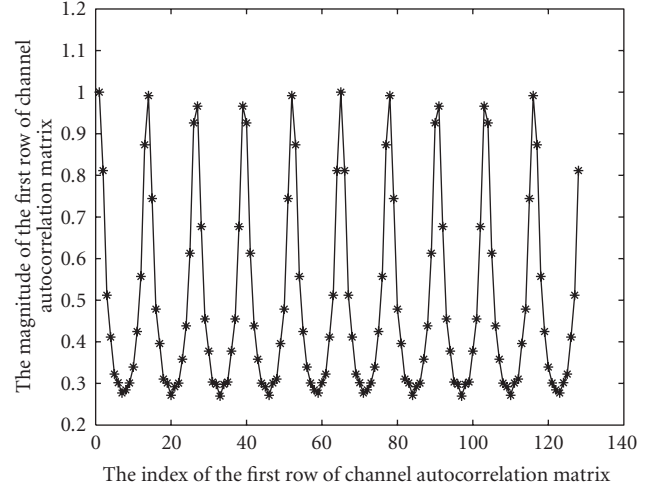


FIGURE 3: The first row of the channel autocorrelation matrix  $\mathbf{R}_{H_p, H_p}$ ,  $\mathbf{A}$ .

The proposed fast LMMSE algorithm avoids the matrix inverse operation and can be very efficient since the algorithm only uses the FFT and circle shift operation. The proposed fast LMMSE algorithm can be summarized as follows.

*Step 1.* Obtain the LS channel estimation of pilot signal in time domain,  $\tilde{h}_{p,ls}(i, k)$ , by formula (14).

*Step 2.* Calculate the average power of each tap for  $N_{MST}$  OFDM symbols,  $P_{LS}(k)$ , by formula (15). Then, we choose the  $L'$  most significant taps from  $P_{LS}(k)$  and reserve it as  $P_{MST}(k)$ , by formula (18).

*Step 3.* Obtain the estimate of SNR,  $\widehat{\text{SNR}}$ , by formula (19).

*Step 4.* Obtain the estimate of the first row of the LMMSE matrix,  $\tilde{\tilde{\mathbf{B}}}$ , by formula (20).

*Step 5.* Obtain the estimation of the LMMSE matrix,  $\tilde{\mathbf{R}}_{H_p, H_p}(\tilde{\mathbf{R}}_{H_p, H_p} + (\beta/\widehat{\text{SNR}})\mathbf{I})^{-1}$ , by circle shift of  $\tilde{\tilde{\mathbf{B}}}$ . Then, the channel estimation in frequency domain at pilot subcarriers can be obtained by formula (21).

It is noted that the estimation of the LMMSE matrix requires only  $N_p$  points FFT operation and circle shifting operation, which reduce the computational complexity significantly compared with the conventional LMMSE estimator since it requires the inverse operation of a large dimension matrix.

#### 4. Analysis of the Mean Square Error of the Proposed Fast LMMSE Algorithm

In this section, we will present the mean square error (MSE) of the proposed fast LMMSE algorithm. Firstly, we present

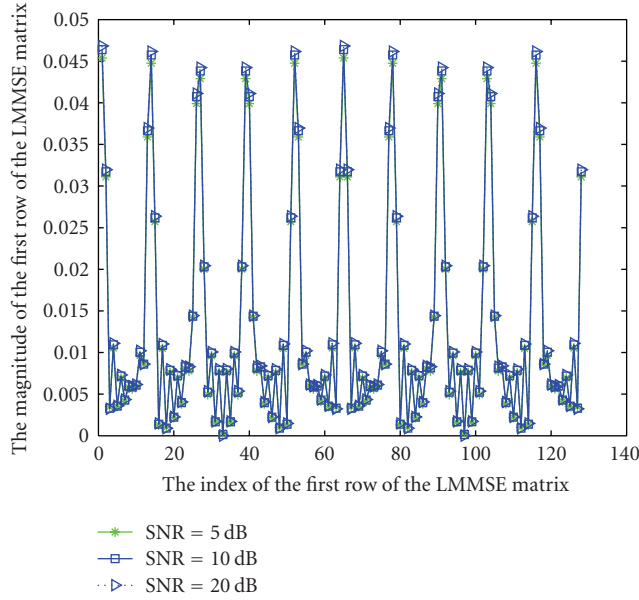


FIGURE 4: The first row of the LMMSE matrix  $\mathbf{R}_{H_p H_p} (\mathbf{R}_{H_p H_p} + (\beta/\text{SNR})\mathbf{I})^{-1}$  with different SNRs.

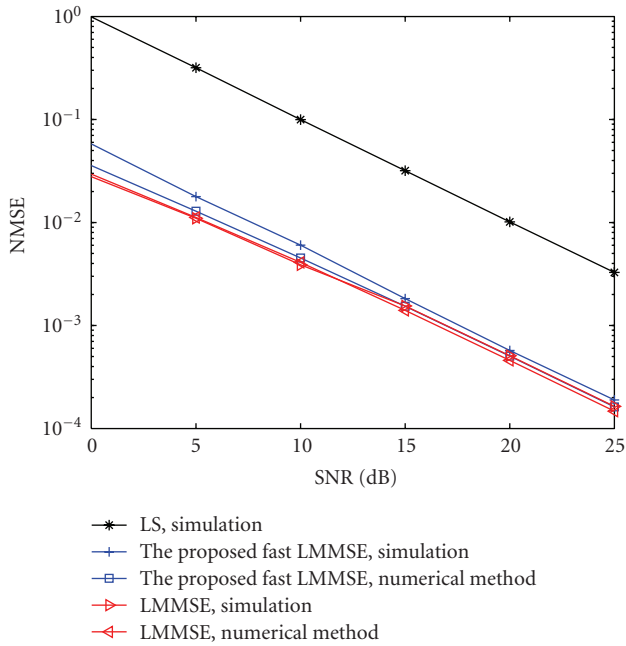


FIGURE 5: Normalized Mean square error (NMSE) of channel estimation of LMMSE algorithm versus that of the proposed fast LMMSE algorithm by computer simulation and numerical method.

the MSE of LMMSE algorithm for comparison. We study two cases. One case is the MSE analysis for matched SNR, that is, the designed SNR is equal to the true SNR, and the other one is the MSE analysis for mismatched SNR. Secondly, we present the MSE of the proposed fast LMMSE algorithm. Similarly, we study two cases. One is for matched SNR, and the other is for mismatched SNR.

**4.1. MSE Analysis of the Conventional LMMSE Algorithm.** Denote the MSE of LMMSE algorithm by  $\varphi_{\text{MSE}}(\text{SNR}, \text{SNR}_{\text{design}})$ , where  $\text{SNR}$  is the true SNR, and  $\text{SNR}_{\text{design}}$  is the designed SNR.

(i) *MSE Analysis for Matched SNR.* The MSE of LMMSE algorithm at pilot subcarriers for matched SNR can be derived as [22]

$$\begin{aligned} \varphi_{\text{MSE}}(\text{SNR}, \text{SNR}) &= \frac{1}{N_p} \sum_{k=0}^{N_p-1} E \left| \tilde{H}_{p, \text{LMMSE}}(i, k) - H_p(i, k) \right|^2 \\ &= 1 - \mathbf{A} \cdot \left( (\mathbf{R}_{H_p H_p})^H + \frac{\beta}{\text{SNR}} \mathbf{I} \right)^{-1} \cdot \mathbf{A}^H, \end{aligned} \quad (22)$$

where  $\mathbf{A}$  is the first row of the matrix  $\mathbf{R}_{H_p H_p}$ , and  $(\cdot)^H$  denotes Hermitian transpose.

(ii) *MSE Analysis for Mismatched SNR.* The MSE of LMMSE algorithm on pilot subcarriers for mismatched SNR can be derived as [22]

$$\begin{aligned} \varphi_{\text{MSE}}(\text{SNR}, \text{SNR}_{\text{design}}) &= \frac{1}{N_p} \sum_{k=0}^{N_p-1} E \left| \tilde{H}_{p, \text{LMMSE}}(i, k) - H_p(i, k) \right|^2 \\ &= 1 + \mathbf{A} \cdot \left( \mathbf{R}_{H_p H_p} + \frac{\beta}{\text{SNR}_{\text{design}}} \mathbf{I} \right)^{-1} \\ &\quad \cdot \left( \mathbf{R}_{H_p H_p} + \frac{\beta}{\text{SNR}} \mathbf{I} \right) \\ &\quad \cdot \left( (\mathbf{R}_{H_p H_p})^H + \frac{\beta}{\text{SNR}_{\text{design}}} \mathbf{I} \right)^{-1} \cdot \mathbf{A}^H \\ &\quad - 2\mathbf{A} \cdot \left( (\mathbf{R}_{H_p H_p})^H + \frac{\beta}{\text{SNR}_{\text{design}}} \mathbf{I} \right)^{-1} \cdot \mathbf{A}^H, \end{aligned} \quad (23)$$

where  $\mathbf{A}$  is the first row of the matrix  $\mathbf{R}_{H_p H_p}$ , and  $(\cdot)^H$  denotes Hermitian transpose.

**4.2. MSE Analysis for the Proposed Fast LMMSE Algorithm.** Let us denote the MSE of the proposed fast LMMSE algorithm by  $\varphi_{\text{MSE}}(\text{SNR}, \widehat{\text{SNR}})$ , where  $\text{SNR}$  is the true SNR, and  $\widehat{\text{SNR}}$  is the estimated SNR or the designed SNR.

(i) *MSE for Matched SNR.* The MSE of the proposed fast LMMSE algorithm is given by

$$\begin{aligned}
 \phi_{\text{MSE}}(\text{SNR}, \text{SNR}) &= E \left[ \frac{1}{N_p} \sum_{k=0}^{N_p-1} \left| \tilde{H}_{p,\text{fast LMMSE}}(i, k) - H_p(i, k) \right|^2 \right] \\
 &= E \left[ \left| \tilde{H}_{p,\text{fast LMMSE}}(i, 0) - H_p(i, 0) \right|^2 \right] \\
 &= E \left[ \left| \sum_{k=0}^{N_p-1} \left\{ \frac{1}{N_p} \sum_{l=0}^{N_p-1} \gamma(l) \exp \left\{ j \frac{2\pi}{N_p} l k \right\} \tilde{H}_{p,\text{ls}}(i, k) \right\} \right. \right. \\
 &\quad \left. \left. - H_p(i, 0) \right|^2 \right] \\
 &= E \left[ \left| \sum_{l=0}^{N_p-1} \gamma(l) \left\{ \frac{1}{N_p} \sum_{k=0}^{N_p-1} \exp \left\{ j \frac{2\pi}{N_p} l k \right\} \tilde{H}_{p,\text{ls}}(i, k) \right\} \right. \right. \\
 &\quad \left. \left. - H_p(i, 0) \right|^2 \right] \\
 &= E \left[ \left| \sum_{l=0}^{N_p-1} \gamma(l) \tilde{h}_{p,\text{ls}}(i, l) - H_p(i, 0) \right|^2 \right] \\
 &= E \left[ \left| \sum_{l=0}^{N_p-1} \gamma(l) \tilde{h}_{p,\text{ls}}(i, l) - \sum_{j=0}^{N_p-1} h_p(i, j) \right|^2 \right],
 \end{aligned} \tag{24}$$

where  $\gamma(l) = (P_{\text{MST}}(l))/(P_{\text{MST}}(l) + (\beta/(N_p \cdot \text{SNR})))$ ,  $l = 0, 1, \dots, N_p - 1$ . If the number of the chosen OFDM symbol to obtain the estimated average power for each tap,  $N_{\text{MST}}$ , is large, we can replace  $\gamma(l)$  with  $E(\gamma(l))$  in (24), then, (24) can be further derived as

$$\begin{aligned}
 \phi_{\text{MSE}}(\text{SNR}, \text{SNR}) &= E \left[ \left| \sum_{l=0}^{N_p-1} E[\gamma(l)] \tilde{h}_{p,\text{ls}}(i, l) - \sum_{j=0}^{N_p-1} h_p(i, j) \right|^2 \right] \\
 &\approx E \left[ \left| \sum_{l=0}^{N_p-1} \frac{E \left( \left| \tilde{h}_{p,\text{MST}}(l) \right|^2 \right)}{E \left( \left| \tilde{h}_{p,\text{MST}}(l) \right|^2 \right) + (\beta/(N_p \cdot \text{SNR}))} \tilde{h}_{p,\text{ls}}(i, l) \right. \right. \\
 &\quad \left. \left. - \sum_{j=0}^{N_p-1} h_p(i, j) \right|^2 \right].
 \end{aligned} \tag{25}$$

If the improved MST algorithm chooses  $L'$  ( $L' \geq L$ ) paths, where  $L$  is number of resolvable paths of the dispersive channel, and the chosen  $L'$  paths contain all the  $L$  channel paths without omission, then (25) can be further written as

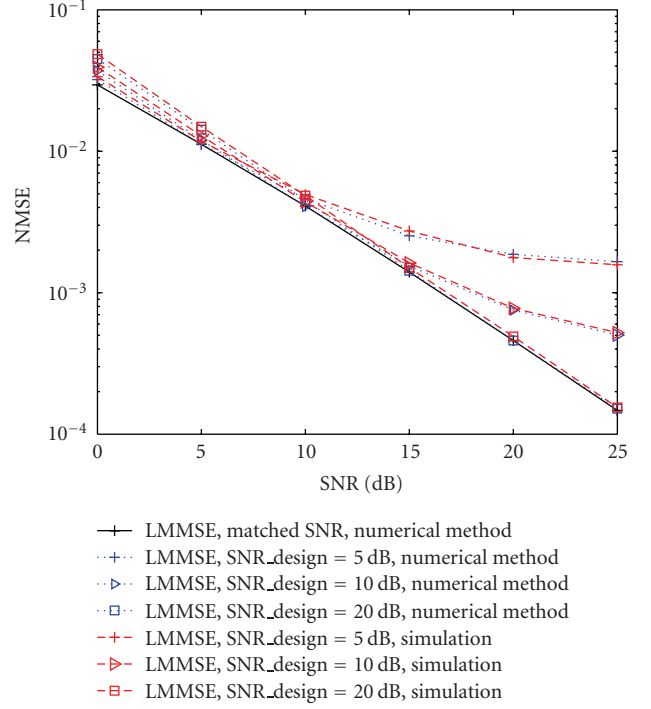


FIGURE 6: NMSE of LMMSE algorithm with matched SNR and mismatched SNRs versus SNR, by simulation and numerical method, respectively.

$$\begin{aligned}
 \phi_{\text{MSE}}(\text{SNR}, \text{SNR}) &= E \left[ \left| \sum_{j=0}^{N_p-1} \frac{E \left( \left| \tilde{h}_{p,\text{MST}}(j) \right|^2 \right)}{E \left( \left| \tilde{h}_{p,\text{MST}}(j) \right|^2 \right) + (\beta/(N_p \cdot \text{SNR}))} \right. \right. \\
 &\quad \left. \left. \times \tilde{h}_{p,\text{ls}}(i, j) - \sum_{j=0}^{N_p-1} h_p(i, j) \right|^2 \right] \\
 &= 1 + \sum_{l=0}^{L-1} |\gamma_1(\tau_l)|^2 \left( \sigma_l^2 + \frac{1}{\text{SNR} \cdot N_p} \right) \\
 &\quad + (L' - L) \left( \frac{(1/(\text{SNR} \cdot N_p))}{(1/(\text{SNR} \cdot N_p)) + (\beta/(\text{SNR} \cdot N_p))} \right)^2 \\
 &\quad \times \frac{1}{\text{SNR} \cdot N_p} - 2 \sum_{l=0}^{L-1} \gamma_1(\tau_l) \sigma_l^2 \\
 &= 1 + \sum_{l=0}^{L-1} |\gamma_1(\tau_l)|^2 \left( \sigma_l^2 + \frac{1}{\text{SNR} \cdot N_p} \right) \\
 &\quad + (L' - L) \left( \frac{1/\text{SNR}}{(1/\text{SNR}) + (\beta/\text{SNR})} \right)^2 \frac{1}{\text{SNR} \cdot N_p} \\
 &\quad - 2 \sum_{l=0}^{L-1} \gamma_1(\tau_l) \sigma_l^2,
 \end{aligned} \tag{26}$$

where  $\tau_l$  is the channel delay of the  $l$ th resolvable path, and  $\sigma_l^2$  is the power of the  $l$ th path,

$$\gamma_1(i) = \begin{cases} \frac{\sigma_l^2 + (1/(\text{SNR} \cdot N_p))}{\sigma_l^2 + (1/(\text{SNR} \cdot N_p)) + (\beta/(\text{SNR} \cdot N_p))}, & \text{if } i \in \alpha, \\ \frac{1/\text{SNR}}{(1/\text{SNR}) + (\beta/\text{SNR})}, & \text{if } i \notin \alpha, \end{cases}$$

$$\alpha = \{\tau_l : l = 0, 1, \dots, L-1\}. \quad (27)$$

(ii) *MSE for Mismatched SNR.* Similarly, the MSE of the proposed fast LMMSE algorithm for mismatched SNR is given by

$$\begin{aligned} & \phi_{\text{MSE}}(\text{SNR}, \widetilde{\text{SNR}}) \\ &= E \left[ \left| \sum_{l=0}^{N_p-1} \gamma'(l) \tilde{h}_{p,ls}(i, l) - \sum_{j=0}^{N_p-1} h_p(i, j) \right|^2 \right] \\ &= 1 + \sum_{l=0}^{L-1} |\gamma_2(\tau_l)|^2 \left( \sigma_l^2 + \frac{1}{\text{SNR} \cdot N_p} \right) \\ &+ (L-1) \left( \frac{1/\text{SNR}}{(1/\text{SNR}) + (\beta/\widetilde{\text{SNR}})} \right)^2 \frac{1}{\text{SNR} \cdot N_p} \\ &- 2 \sum_{l=0}^{L-1} \gamma_2(\tau_l) \sigma_l^2, \end{aligned} \quad (28)$$

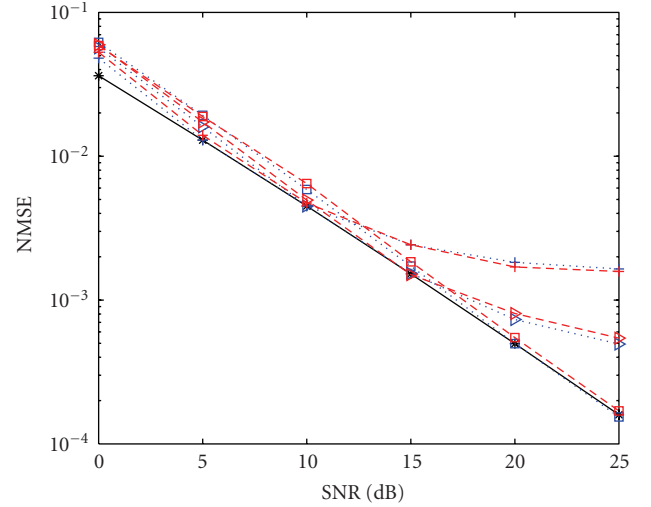
where  $\gamma'(l) = P_{\text{MST}}(l)/(P_{\text{MST}}(l) + (\beta/(N_p \widetilde{\text{SNR}})))$ ,  $l = 0, 1, \dots, N_p - 1$ .  $\tau_l$  is the channel delay of the  $l$ th resolvable path, and  $\sigma_l^2$  is the power of the  $l$ th path,

$$\gamma_2(i) = \begin{cases} \frac{\sigma_l^2 + (1/(\text{SNR} \cdot N_p))}{\sigma_l^2 + (1/(\text{SNR} \cdot N_p)) + (\beta/(\widetilde{\text{SNR}} \cdot N_p))}, & \text{if } i \in \alpha, \\ \frac{1/\text{SNR}}{(1/\text{SNR}) + (\beta/\widetilde{\text{SNR}})}, & \text{if } i \notin \alpha, \end{cases}$$

$$\alpha = \{\tau_l : l = 0, 1, \dots, L-1\}. \quad (29)$$

It is noted that since the channel is assumed to be normalized, the MSE of the proposed fast LMMSE algorithm and the MSE of the conventional LMMSE are equal to their normalized mean square errors (NMSEs), respectively. In addition, for the sake of performance comparison between the above analysis of NMSE and the NMSE obtained by computer simulation, we define the NMSE obtained by simulation as follows:

$$\text{NMSE}_{\text{simu}} = \frac{\sum_{i=0}^{K-1} \sum_{j=0}^{N_p-1} |\tilde{H}_p(i, j) - H_p(i, j)|^2}{\sum_{i=0}^{K-1} \sum_{j=0}^{N_p-1} |H_p(i, j)|^2}, \quad (30)$$



—\*— The proposed fast LMMSE, matched SNR, numerical method  
 ···+·· The proposed fast LMMSE, SNR\_design = 5 dB, numerical method  
 ···△·· The proposed fast LMMSE, SNR\_design = 10 dB, numerical method  
 ···□·· The proposed fast LMMSE, SNR\_design = 20 dB, numerical method  
 -+-+ The proposed fast LMMSE, SNR\_design = 5 dB, simulation  
 -+△- The proposed fast LMMSE, SNR\_design = 10 dB, simulation  
 -+□- The proposed fast LMMSE, SNR\_design = 20 dB, simulation

FIGURE 7: NMSE of the proposed fast LMMSE algorithm with matched SNR and mismatched SNRs versus SNR, by simulation and numerical method, respectively.

where  $\tilde{H}_p(i, j)$  denotes the channel estimate at the  $j$ th pilot subcarrier in the  $i$ th OFDM symbol, obtained by LMMSE algorithm or the proposed fast LMMSE algorithm, and  $K$  denotes the number of OFDM symbols in the simulation.

## 5. Numerical and Simulation Results

Both computer simulation and numerical method have been deployed to investigate the performance of the proposed fast LMMSE algorithm for channel estimation. In the simulation, we employ the channel model of COST207 [23] having 6 numbers of paths, that is,  $L = 6$ , and the maximum delay spread of 2.5 microseconds. The channel power intensity profile is listed in Table 1. The number of the subcarriers of the OFDM system,  $N$ , is equal to 2048, and the CP length is equal to 128 sample points. The bandwidth of the system is 20 MHz so that one OFDM symbol period  $T_s = 102.4$  microseconds and the CP period  $T_{CP} = 6.4$  microseconds  $>$  2.5 microseconds. The number of the total pilots  $N_p$  is equal to 128, and the pilot gap  $R$  is 16. The transmitted signal is BPSK modulated, and the Doppler shift is 100 Hz.

### 5.1. Channel Autocorrelation Matrix under Different SNRs.

Figure 3 shows the magnitude of the first row of the channel autocorrelation matrix  $\mathbf{R}_{H_p, H_p}$ ,  $\mathbf{A}$ . Since the channel autocorrelation matrix is circulant, it is enough to show the first row of the channel autocorrelation matrix. Observe that the magnitude of  $\mathbf{A}$  varies approximately periodically, and the period is 13 pilot subcarriers. Since the channel

power intensity profile is negative exponential distributed, the period of the first row of the channel autocorrelation matrix is decided by the delay of the second path. The delay of the second path is 0.5 microseconds, that is, 10 sample points. According to (7), the period is  $N_p/\tau_1 = 128/10 = 12.8$ . It is noted that the parameter  $N$  should be replaced by  $N_p$  in (7). Therefore, the period is about 13, as shown in Figure 3. Figure 4 shows the magnitude of the first row of the LMMSE matrix  $\mathbf{R}_{\mathbf{H}_p\mathbf{H}_p}(\mathbf{R}_{\mathbf{H}_p\mathbf{H}_p} + (\beta/\text{SNR})\mathbf{I})^{-1}$  with SNR of 5 dB, 10 dB, and 20 dB, respectively. Since the LMMSE matrix is also circulant, it is sufficient to depict the first row of the LMMSE matrix. Observe that the value of the first row of the LMMSE matrix is symmetry, and the center point is 64. The first row of the LMMSE matrix is approximately periodic, and the period is about 13 pilot subcarriers. Observe that the value of the first row of the LMMSE matrix varies insignificantly when SNR changes from 5 dB to 20 dB. In addition, the local maximum values of the curves correspond to strong correlation between pilot subcarriers, and the local minimum values correspond to weak correlation between pilot subcarriers.

**5.2. Normalized Mean Square Error (NMSE) Comparison of Channel Estimation between LMMSE Algorithm and the Proposed Fast LMMSE Algorithm.** Figure 5 shows the NMSE of channel estimation of LMMSE algorithm versus that of the proposed fast LMMSE algorithm by computer simulation and numerical method, respectively. The numerical results of LMMSE algorithm and the proposed fast LMMSE algorithm are obtained by (22) and (26), respectively. The simulation results are obtained by (30). We replace  $\tilde{\mathbf{H}}_p$  in (30) with  $\tilde{\mathbf{H}}_{p,\text{LMMSE}}$  for LMMSE algorithm and replace  $\tilde{\mathbf{H}}_p$  with  $\tilde{\mathbf{H}}_{p,\text{fast LMMSE}}$  for the proposed fast LMMSE algorithm, respectively. For the proposed fast LMMSE algorithm, the number of OFDM symbols chosen to obtain the average power of each tap,  $N_{\text{MST}}$ , is 20, and the number of chosen paths,  $L'$ , is 10. The number of OFDM symbols in the simulation,  $K$ , is 5000, for both LMMSE algorithm and the proposed fast LMMSE algorithm. Observe that the NMSE of the proposed fast LMMSE algorithm is very close to that of LMMSE algorithm in theory over the SNR range from 0 dB to 25 dB. In addition, for LMMSE algorithm the numerical result is verified by the simulation. For the proposed fast LMMSE algorithm, the simulation result approaches the numerical result well, except that the simulation result is a little higher than the numerical result at low SNR. Observe that both the proposed fast LMMSE algorithm and LMMSE algorithm are superior to LS algorithm. For instance, the LMMSE algorithm has about 16 dB gain over the LS algorithm, at the same MSE over the SNR range from 0 dB to 25 dB.

Figure 6 shows the normalized mean square error (NMSE) of LMMSE algorithm with matched SNR and mismatched SNRs versus SNR, by simulation and numerical method, respectively. Firstly, we give a necessary illustration of the curves obtained by numerical method. For the curves with matched SNR, we use (22) to calculate the MSEs under different SNRs, by numerical method. For the curves with

TABLE 1: Channel Power Intensity Profile.

Tap	Delay ( $\mu\text{s}$ )	Gain (dB)	Doppler Spectrum
1	0	0.0	Clarke [24]
2	0.5	-6.0	Clarke
3	1.0	-12.0	Clarke
4	1.5	-18.0	Clarke
5	2.0	-24.0	Clarke
6	2.5	-30.0	Clarke

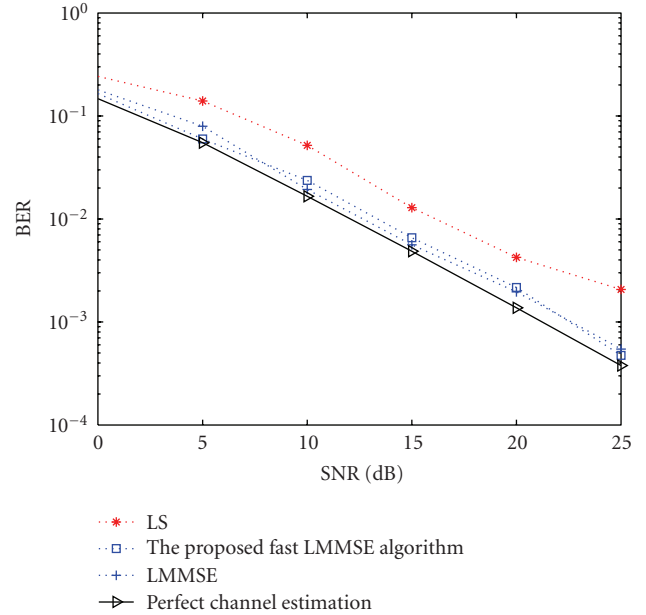


FIGURE 8: Bit error rate (BER) of the LS, LMMSE, the proposed fast LMMSE, and perfect channel estimation versus SNR.

mismatched SNRs, that is, designed SNRs, we use (23) to obtain the results, by numerical method. Secondly, for the curves with mismatched SNRs obtained by computer simulation, we use the designed SNR (predetermined and invariable) instead of the true SNR in (13) to obtain the channel estimation of pilot subcarriers. Observe that the analysis results are verified by computer simulation well, for the designed SNR of 5 dB, 10 dB, and 20 dB, respectively. For the case of the designed SNR of 5 dB, the MSE approaches the curve of matched SNR well within the range from 0 dB to about 10 dB. However, when the SNR increases, an MSE floor of about  $2 \times 10^{-3}$  occurs. Similar trend can be found for the case of designed SNR of 10 dB. Observe that the curve of designed 20 dB approaches the curve with matched SNR well within the SNR range from 0 dB to 25 dB. Therefore, if we only know the channel autocorrelation matrix  $\mathbf{R}_{\mathbf{H}_p\mathbf{H}_p}$  and do not know the SNR, the above results suggest that we use a higher designed SNR in (13) when performing channel estimation.

Figure 7 shows the NMSE of the proposed fast LMMSE algorithm with matched SNR and mismatched SNRs versus SNR, by simulation and numerical method respectively.

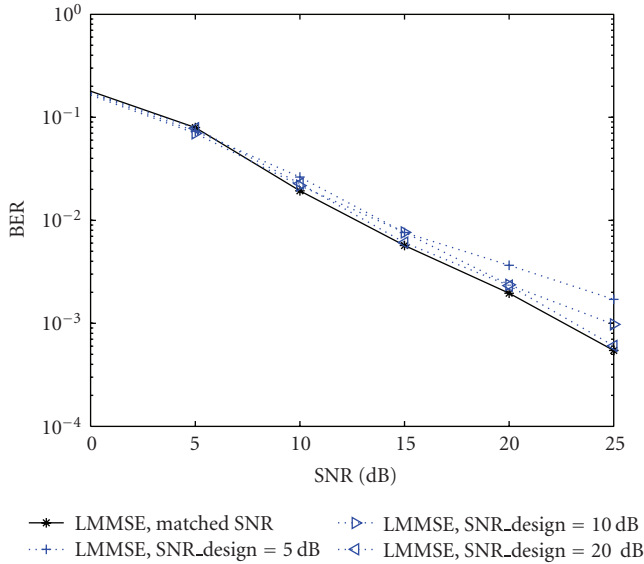


FIGURE 9: BER comparison between LMMSE channel estimation with matched SNR and LMMSE channel estimation with designed SNRs.

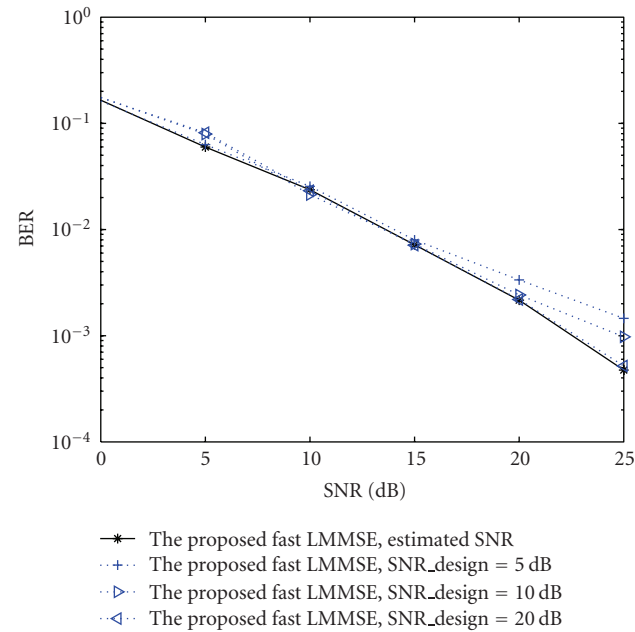


FIGURE 10: BER comparison between the proposed fast LMMSE channel estimation with estimated SNR and the proposed fast LMMSE channel estimation with designed SNRs.

Firstly, we give a brief illustration of the curves obtained by numerical method. For the curve with matched SNR, we use (26) to obtain the results. For the curves with mismatched SNRs, that is, designed SNR, we use (28) to obtain the numerical results. To verify the numerical results, we perform computer simulation for each case with different designed SNR. In the computer simulation, step 3 in the proposed fast LMMSE algorithm is modified by letting the estimated SNR,  $\widehat{\text{SNR}}$ , be the designed SNR. For instance, if

we choose the designed SNR to be 10 dB,  $\widehat{\text{SNR}}$  will be set to be 10 dB in step 3 of the proposed fast LMMSE algorithm instead of using formula (19) to obtain  $\widehat{\text{SNR}}$ . For the computer simulation, the number of OFDM symbols chosen to obtain the average power of each tap,  $N_{\text{MST}}$ , is 20, and the number of chosen paths,  $L'$ , is 10. The number of OFDM symbols in the simulation,  $K$ , is 5000. Observe that the analysis results are verified by computer simulation well, for the designed SNR of 5 dB, 10 dB, and 20 dB, respectively. For the case of the designed SNR of 5 dB, the MSE approaches the curve of matched SNR well within the range from 0 dB to about 10 dB. However, when the SNR increases, an MSE floor of about  $2 \times 10^{-3}$  occurs. Similar trend can be found for the case of designed SNR of 10 dB. Observe that the curve of designed 20 dB approaches the curve of matched SNR well within the SNR range from 0 dB to 25 dB.

**5.3. Bit Error Rate (BER) Comparison between LMMSE Algorithm and the Proposed Fast LMMSE Algorithm.** Figure 8 shows the BER of LS, LMMSE, the proposed fast LMMSE, and perfect channel estimation, respectively. We adopt linear interpolation to obtain the channel frequency response at all subcarriers after the channel frequency response at pilot subcarriers is obtained by LS, LMMSE, and the proposed fast LMMSE estimator. Once the channel frequency response is obtained, we use maximum likelihood detection to obtain the estimated signal  $\tilde{X}(i, k)$ . In addition, the perfect channel estimation refers to that the channel frequency response is known by the receiver in advance. Observe that the BERs of LMMSE estimator is very close to that of the proposed fast LMMSE estimator over the SNR range from 0 dB to 25 dB. And they are about 1 dB worse than the perfect channel estimator, over the SNR ranging from 0 dB to 25 dB. The LMMSE estimator and the proposed LMMSE estimator are about 3–4 dB better than the LS estimator at the same BER over the SNR ranging from 0 dB to 25 dB.

Figure 9 shows the BER performance of the LMMSE channel estimation with matched SNR and the LMMSE channel estimation with designed SNRs. The LMMSE channel estimator with designed SNR refers to that we use a predetermined and unchanged SNR in (13) instead of the true SNR. Observe that the BERs of the LMMSE with designed SNR of 5 dB, 10 dB, and 20 dB are almost overlapped with each other within the lower SNR range from 0 dB to 15 dB. However, when SNR increases from 15 dB to 25 dB, the BER of the LMMSE estimator with higher designed SNR is better than that of the lower designed SNR. The results are consistent with the NMSEs in Figure 4. Therefore, a design for higher SNR is preferable as for mismatch in SNR.

Figure 10 shows the BER of the proposed fast LMMSE estimator with estimated SNR and the proposed fast LMMSE estimator with designed SNRs. It is noted that the proposed fast LMMSE estimator with estimated SNR refers to our proposed algorithm summarized in Section 3. The proposed fast LMMSE estimator with designed SNR refers to that we modify the step 3 of the proposed algorithm by using a predetermined and unchanged SNR instead of using formula

(19) to obtain the estimated SNR. Observe that the BERs of the proposed fast LMMSE estimator with designed SNR of 5 dB, 10 dB, and 20 dB are almost overlapped with each other within the lower SNR range from 0 dB to 15 dB. However, when SNR increases from 15 dB to 25 dB, the BER of the proposed fast LMMSE estimator with higher designed SNR is better than that of the lower designed SNR. Thus, a design for higher SNR is preferable as for mismatch in SNR.

## 6. Conclusion

In this paper, a fast LMMSE channel estimation method has been proposed and thoroughly investigated for OFDM systems. Since the conventional LMMSE channel estimation requires the channel statistics, that is, the channel autocorrelation matrix in frequency domain and SNR, which are often unavailable in practical systems, the application of the conventional LMMSE channel estimation is limited. Our proposed method can efficiently estimate the channel autocorrelation matrix by the improved MST algorithm and calculate the LMMSE matrix by Kumar's fast algorithm and exploiting the property of the channel autocorrelation matrix so that the computation complexity can be reduced significantly. We present the MSE analysis for the proposed method and the conventional LMMSE method and investigate the MSE thoroughly under two cases, that is, the matched SNR and the mismatched SNR. Numerical results and computer simulation show that a design for higher SNR is preferable as for mismatch in SNR.

## Appendices

### A.

In this appendix, we will prove that the rank of  $\mathbf{R}_{\text{HH}}$  is equal to  $L$  and the rank of  $\mathbf{R}_{\text{HH}} + \sigma_w^2 \mathbf{I}$  is equal to  $N$ . We can obtain from (7) and (9) that

$$\begin{aligned} \lambda_k &= \sum_{n=0}^{N-1} R_{\text{HH}}(0, n) \exp\left\{-\frac{j2\pi nk}{N}\right\} \\ &= \sum_{n=0}^{N-1} \sum_{l=0}^{L-1} \sigma_l^2 \exp\left\{\frac{j2\pi \tau_l n}{N}\right\} \exp\left\{-\frac{j2\pi nk}{N}\right\} \\ &= \begin{cases} 0, & \text{for } k \notin \alpha, \\ N \sum_{l=0}^{L-1} \sigma_l^2, & \text{for } k \in \alpha, \end{cases} \quad (\text{A.1}) \\ &= \begin{cases} 0, & \text{for } k \notin \alpha, \\ N, & \text{for } k \in \alpha, \end{cases} \end{aligned}$$

where  $\alpha = \{\tau_l \mid l = 0, 1, \dots, L-1\}$ ,  $\tau_l$  is the delay of the  $l$ th path, and  $L$  is the number of resolvable paths. Thus, the number of nonzero eigenvalues of  $\mathbf{R}_{\text{HH}}$  is equal to  $L$ .

Denote the eigenvalues of the matrix  $\mathbf{R}_{\text{HH}} + \sigma_w^2 \mathbf{I}$  by  $\mu_k$ ,  $k = 0, 1, \dots, N-1$ . We can obtain that

$$\begin{aligned} & \left[ \mu_0 \quad \mu_1 \quad \cdots \quad \mu_{N-1} \right] \\ &= \left[ \text{FFT}_N(R_{\text{HH}}(0, 0) + \sigma_w^2) \quad R_{\text{HH}}(0, 1) \quad \cdots \quad R_{\text{HH}}(0, N-1) \right] \\ &= \left[ \lambda_0 + \sigma_w^2 \quad \lambda_1 + \sigma_w^2 \quad \cdots \quad \lambda_{N-1} + \sigma_w^2 \right]. \end{aligned} \quad (\text{A.2})$$

Therefore the number of nonzero eigenvalues of the matrix  $\mathbf{R}_{\text{HH}} + \sigma_w^2 \mathbf{I}$  is  $N$  and the rank of the matrix  $\mathbf{R}_{\text{HH}} + \sigma_w^2 \mathbf{I}$  is  $N$ .

### B.

In this appendix, we will show the derivation of (20). Since the matrix  $\tilde{\mathbf{R}}_{\text{H}_p \text{H}_p} + (\beta/\widehat{\text{SNR}})\mathbf{I}$  is circulant, the inverse matrix  $(\tilde{\mathbf{R}}_{\text{H}_p \text{H}_p} + (\beta/\widehat{\text{SNR}})\mathbf{I})^{-1}$  can be obtained by Kumar's fast algorithm [25]. Denote the first row of  $\tilde{\mathbf{R}}_{\text{H}_p \text{H}_p} + (\beta/\widehat{\text{SNR}})\mathbf{I}$  by  $\mathbf{C}$ , and we have

$$\mathbf{C} = \left[ \tilde{R}_{\text{H}_p \text{H}_p}(0, 0) + \frac{\beta}{\widehat{\text{SNR}}} \quad \tilde{R}_{\text{H}_p \text{H}_p}(0, 1) \quad \cdots \quad \tilde{R}_{\text{H}_p \text{H}_p}(0, N_p - 1) \right]. \quad (\text{B.3})$$

Kumar's fast algorithm can be summarized as follows.

*Step 1.* Compute  $N_p$  points FFT of the vector  $\mathbf{C}$  and we obtain

$$\mathbf{D} = [d_0 \quad d_1 \quad \cdots \quad d_{N_p-1}] = \text{FFT}_{N_p}(\mathbf{C}). \quad (\text{B.4})$$

*Step 2.*  $\mathbf{E}$  can be obtained from (B.4) as

$$\mathbf{E} = \left[ \frac{1}{d_0} \quad \frac{1}{d_1} \quad \cdots \quad \frac{1}{d_{N_p-1}} \right]. \quad (\text{B.5})$$

*Step 3.* Denote the first row of the matrix  $(\tilde{\mathbf{R}}_{\text{H}_p \text{H}_p} + (\beta/\widehat{\text{SNR}})\mathbf{I})^{-1}$  by  $\mathbf{F}$ , and  $\mathbf{F}$  can be given by computing  $N_p$  points IFFT of the vector  $\mathbf{E}$ :

$$\mathbf{F} = \text{IFFT}_{N_p}(\mathbf{E}). \quad (\text{B.6})$$

The above three steps can be combined as

$$\mathbf{F} = \text{IFFT}_{N_p} \left( \mathbf{1} \cdot \left[ \text{diag}\{\text{FFT}_{N_p}(\mathbf{C})\} \right]^{-1} \right), \quad (\text{B.7})$$

where  $\mathbf{1} = [1 \ 1 \ \cdots \ 1]_{1 \times N_p}$ , and  $\text{diag}\{\bullet\}$  denotes diagonalization operation. The matrix  $(\tilde{\mathbf{R}}_{\text{H}_p \text{H}_p} + (\beta/\widehat{\text{SNR}})\mathbf{I})^{-1}$  can be acquired from the  $\mathbf{1}$  by  $N_p$  vector  $\mathbf{F}$  by circle shift. Denote

the first row of the matrix  $\tilde{\mathbf{R}}_{\mathbf{H}_p, \mathbf{H}_p} (\tilde{\mathbf{R}}_{\mathbf{H}_p, \mathbf{H}_p} + (\beta/\overline{\text{SNR}})\mathbf{I})^{-1}$  by  $\tilde{\mathbf{B}}$ , the first column of the matrix  $(\tilde{\mathbf{R}}_{\mathbf{H}_p, \mathbf{H}_p} + (\beta/\overline{\text{SNR}})\mathbf{I})^{-1}$  by  $\tilde{\mathbf{G}}$ . It follows that

$$\tilde{B}(j) = \sum_{i=0}^{N_p-1} \tilde{A}(i) \tilde{G}((i-j) \bmod N_p), \quad j = 0, 1, \dots, N_p - 1, \quad (\text{B.8})$$

where  $\tilde{B}(i)$ ,  $\tilde{A}(i)$ , and  $\tilde{G}(i)$  are the  $i$ th elements of the vector  $\tilde{\mathbf{B}}$ ,  $\tilde{\mathbf{A}}$ , and  $\tilde{\mathbf{G}}$ , respectively.  $\tilde{\mathbf{A}}$  is the first row of the matrix  $\tilde{\mathbf{R}}_{\mathbf{H}_p, \mathbf{H}_p}$ . Since  $\tilde{\mathbf{G}} = \mathbf{F}^H$  and  $\tilde{G}(i) = G^*(N_p - i)$ , where  $(\bullet)^*$  denote conjugate,  $(\bullet)^H$  denotes Hermitian transpose, and (B.8) can be equivalently written as

$$\tilde{B}(j) = \sum_{i=0}^{N_p-1} \tilde{A}(i) F((j-i) \bmod N_p), \quad j = 0, 1, \dots, N_p - 1. \quad (\text{B.9})$$

Or equivalently,

$$\tilde{\mathbf{B}} = \tilde{\mathbf{A}} \otimes \mathbf{F}, \quad (\text{B.10})$$

where  $\otimes$  denotes circulant convolution, and  $F(i)$  is the  $i$ th entry of the vector  $\mathbf{F}$ . Using the property of DFT, (B.10) can be written as

$$\begin{aligned} \tilde{\mathbf{B}} &= \tilde{\mathbf{A}} \otimes \mathbf{F} \\ &= \text{IFFT}_{N_p} \left\{ \text{FFT}_{N_p} \left[ \tilde{\mathbf{A}} \cdot \mathbf{1} \cdot \left[ \text{diag} \left\{ \text{FFT}_{N_p}(\mathbf{F}) \right\} \right]^{-1} \right] \right\}. \end{aligned} \quad (\text{B.11})$$

Using (17), (B.3), and (B.7), (B.11) can be further written as

$$\begin{aligned} \tilde{\mathbf{B}} &= \\ \text{IFFT}_{N_p} &\left[ \frac{P_{\text{MST}}(0)}{P_{\text{MST}}(0) + (\beta/(N_p \overline{\text{SNR}}))} \frac{P_{\text{MST}}(1)}{P_{\text{MST}}(1) + (\beta/(N_p \overline{\text{SNR}}))} \right. \\ &\quad \left. \cdots \frac{P_{\text{MST}}(N_p - 1)}{P_{\text{MST}}(N_p - 1) + (\beta/(N_p \overline{\text{SNR}}))} \right]. \end{aligned} \quad (\text{B.12})$$

## References

- [1] S. B. Weinstein and P. M. Ebert, "Data transmission by frequency-division multiplexing using the discrete Fourier transform," *IEEE Transactions on Communications*, vol. 19, no. 5, part 1, pp. 628–634, 1971.
- [2] D. S. W. Hui, V. K. N. Lau, and W. H. Lam, "Cross-layer design for OFDMA wireless systems with heterogeneous delay requirements," *IEEE Transactions on Wireless Communications*, vol. 6, no. 8, pp. 2872–2880, 2007.
- [3] S. Coleri, M. Ergen, A. Puri, and A. Bahai, "Channel estimation techniques based on pilot arrangement in OFDM systems," *IEEE Transactions on Broadcasting*, vol. 48, no. 3, pp. 223–229, 2002.
- [4] M.-H. Hsieh and C.-H. Wei, "Channel estimation for OFDM systems based on comb-type pilot arrangement in frequency selective fading channels," *IEEE Transactions on Consumer Electronics*, vol. 44, no. 1, pp. 217–225, 1998.
- [5] Y. Zeng, W. H. Lam, and T. S. Ng, "Semiblind channel estimation and equalization for MIMO space-time coded OFDM," *IEEE Transactions on Circuits and Systems I*, vol. 53, no. 2, pp. 463–473, 2006.
- [6] O. Edfors, M. Sandell, J.-J. van de Beek, S. K. Wilson, and P. O. Börjesson, "OFDM channel estimation by singular value decomposition," *IEEE Transactions on Communications*, vol. 46, no. 7, pp. 931–939, 1998.
- [7] O. Simeone, Y. Bar-Ness, and U. Spagnolini, "Pilot-based channel estimation for OFDM systems by tracking the delay-subspace," *IEEE Transactions on Wireless Communications*, vol. 3, no. 1, pp. 315–325, 2004.
- [8] Y. Zhao and A. Huang, "A novel channel estimation method for OFDM mobile communication systems based on pilot signals and transform-domain processing," in *Proceedings of the 47th IEEE Vehicular Technology Conference (VTC '97)*, vol. 3, pp. 2089–2093, Phoenix, Ariz, USA, May 1997.
- [9] J.-C. Lin, "Least-squares channel estimation for mobile OFDM communication on time-varying frequency-selective fading channels," *IEEE Transactions on Vehicular Technology*, vol. 57, no. 6, pp. 3538–3550, 2008.
- [10] R. Lin and A. P. Petropulu, "Linear precoding assisted blind channel estimation for OFDM systems," *IEEE Transactions on Vehicular Technology*, vol. 54, no. 3, pp. 983–995, 2005.
- [11] X. D. Cai and A. N. Akansu, "A subspace method for blind channel identification in OFDM systems," in *Proceedings of the IEEE International Conference on Communications (ICC '00)*, vol. 2, pp. 929–933, New Orleans, La, USA, June 2000.
- [12] X. G. Doukopoulos and G. V. Moustakides, "Blind adaptive channel estimation in OFDM systems," *IEEE Transactions on Wireless Communications*, vol. 5, no. 7, pp. 1716–1725, 2006.
- [13] S. Coleri, M. Ergen, A. Puri, and A. Bahai, "A study of channel estimation in OFDM systems," in *Proceedings of the 56th IEEE Vehicular Technology Conference (VTC '02)*, vol. 2, pp. 894–898, Vancouver, Canada, September 2002.
- [14] J.-J. van de Beek, O. Edfors, M. Sandell, S. K. Wilson, and P. O. Börjesson, "On channel estimation in OFDM systems," in *Proceedings of the 45th IEEE Vehicular Technology Conference (VTC '95)*, vol. 2, pp. 815–819, Chicago, Ill, USA, July 1995.
- [15] Y. Li, L. J. Cimini Jr., and N. R. Sollenberger, "Robust channel estimation for OFDM systems with rapid dispersive fading channels," *IEEE Transactions on Communications*, vol. 46, no. 7, pp. 902–915, 1998.
- [16] M. Morelli and U. Mengali, "A comparison of pilot-aided channel estimation methods for OFDM systems," *IEEE Transactions on Signal Processing*, vol. 49, no. 12, pp. 3065–3073, 2001.
- [17] C. Kuo and J.-F. Chang, "Equalization and channel estimation for OFDM systems in time-varying multipath channels," in *Proceedings of the 15th IEEE International Symposium on Personal, Indoor and Mobile Radio Communications (PIMRC '04)*, vol. 1, pp. 474–478, Barcelona, Spain, September 2004.
- [18] W.-G. Song and J.-T. Lim, "Channel estimation and signal detection for MIMO-OFDM with time varying channels," *IEEE Communications Letters*, vol. 10, no. 7, pp. 540–542, 2006.
- [19] M. J. Fernández-Getino García, J. M. Páez-Borrillo, and S. Zazo, "DFT-based channel estimation in 2D-pilot-symbol-aided OFDM wireless systems," in *Proceedings of the 53rd IEEE Vehicular Technology Conference (VTC '01)*, vol. 2, pp. 810–814, Rhodes, Greece, May 2001.
- [20] A. Böttcher and S. M. Grudsky, *Spectral Properties of Banded Toeplitz Matrices*, SIAM, Philadelphia, Pa, USA, 2005.

- [21] H. Minn and V. K. Bhargava, "An investigation into time-domain approach for OFDM channel estimation," *IEEE Transactions on Broadcasting*, vol. 46, no. 4, pp. 240–248, 2000.
- [22] S. Haykin, *Adaptive Filter Theory*, Publishing House of Electronics Industry, Beijing, China, 4th edition, 2002.
- [23] M. Failli, "Digital land mobile radio communications—COST 207," Tech. Rep. EUR 12160, Commission of the European Communities, Brussels, Belgium, September 1988.
- [24] T. S. Rappaport, *Wireless Communications Principles and Practice*, Publishing House of Electronics Industry, Beijing, China, 2002.
- [25] R. Kumar, "A fast algorithm for solving a Toeplitz system of equations," *IEEE Transactions on Acoustics, Speech, and Signal Processing*, vol. 33, no. 1, pp. 254–267, 1985.